Analyst

PAPER

Cite this: *Analyst*, 2019, **144**, 6231

A graphene oxide-based fluorescence assay for the sensitive detection of DNA exonuclease enzymatic activity

Xiao Liu,† Yingfen Wu,† Xu Wu * and Julia Xiaojun Zhao*

The 3′–5′ exonuclease enzyme plays a dominant role in multiple pivotal physiological activities, such as DNA replication and repair processes. In this study, we designed a sensitive graphene oxide (GO)-based probe for the detection of exonuclease enzymatic activity. In the absence of Exo III, the strong π–π interaction between the fluorophore-tagged DNA and GO causes the efficient fluorescence quenching *via* a fluorescence resonance energy transfer (FRET). In contrast, in the presence of Exo III, the fluorophore-tagged 3′-hydroxyl termini of the DNA probe was digested by Exo III to set the fluorophore free from adsorption when GO was introduced, causing an inefficient fluorescence quenching. As a result, the fluorescence intensity of the sensor was found to be proportional to the concentration of Exo III; towards the detection of Exo III, this simple GO-based probe demonstrated a highly sensitive and selective linear response in the low detection range from 0.01 U mL^{-1} to 0.5 U mL^{-1} and with the limit of detection (LOD) of 0.001 U mL^{-1}. Compared with other fluorescent probes, this assay exhibited superior sensitivity and selectivity in both buffer and fetal bovine serum samples, in addition to being cost effective and having a simple setup.

Received 9th July 2019,
Accepted 6th September 2019

DOI: 10.1039/c9an01283d

rsc.li/analyst

Introduction

In enzymatic studies, exonuclease families have been involved in the numerous aspects of cellular metabolism and maintenance in physiological processes such as DNA proofreading and the maintenance of genome stability.[1] The 3′–5′ exonuclease III (Exo III), isolated from *E. coli* in 1964, is a key bifunctional enzyme and essential to genome stability. The function of Exo III is to remove mononucleotides from the 3′-hydroxyl termini of double-stranded DNA.[2] In the process of DNA replication, 3′–5′ exonuclease plays indispensable functions such as repairing the DNA breaks,[3] assuring the accuracy of replication process and stabilizing the mutation rates in cells.[4–7] Due to defects in the 3′–5′ exonuclease enzymes, cells process wrong transcription, translation and eventually lack protection from cancer, in particular under a long period of stress.[1,8] Therefore, it is highly desired to develop well-performing analytical methods for the precise measurement of the 3′–5′ exonuclease activity.[9,10]

Traditional methods for the detection of 3′–5′ exonuclease enzymatic activity are based on gel electrophoresis, which requires radioactively labelled DNA probes. However, the liabilities of these methods include time-consuming measurements, tedious steps and safety concerns because of radiographic exposure process.[11–13] To overcome these limitations, a number of fluorescence biosensing systems have been developed due to their simple and cost-effective properties.[14–16] For example, Yang *et al.* designed a label-free, "turn-on" fluorescence assay for the rapid detection of exonuclease III activity based on the Tb^{3+}-promoted G-quadruplex.[17] Zhang's group developed a triple-color fluorescent probe by a lab-on-a-DNA-molecule for the simultaneous detection of multiple exonucleases.[18] Recently, we constructed a dual molecular hairpin system to distinguish various exonucleases rapidly.[19] Compared with the case of traditional methods, both the cost and the complexity of these approaches are significantly less. However, the relatively high background signals and limit of detection constrain the detection of exonuclease activity at low concentrations in a complex matrix.

Graphene oxide (GO), as a universal fluorescence quencher, is a two-dimensional oxidized version of graphite.[20,21] It comprises carbon–carbon sp^2 domains together with multiple functional groups such as carboxylic group, hydroxyl group and epoxide group.[22] One of the most interesting roles of GO in sensing systems is to serve as a universal fluorescence quencher through fluorescence resonance energy transfer (FRET).[23] For example, fluorophore-labeled single-stranded

Department of Chemistry, University of North Dakota, Grand Forks, ND 58202, USA. E-mail: xu.wu@und.edu, julia.zhao@und.edu
† These authors contribute equally to this work.

DNA (ssDNA) molecules can be easily attached onto the surface of GO by the strong π–π stacking interactions between GO and exposed nucleobases, inducing significant fluorescence quenching.[24–29] In contrast, the binding force would become much weaker once the double-stranded DNA (dsDNA) is formed, which releases the fluorophore from the GO and restores the fluorescence. The difference in the binding forces between GO and ssDNA and between GO and dsDNA has been widely used to construct assays for the detection of DNA, proteins, enzymes, metal ions, *etc.*[30] For instance, Min *et al.*[14] used this strategy to construct a fluorescent sensor for detecting the activity of Exo III, in which the fluorescence was significantly decreased in the presence of Exo III. However, the signal "turn-off" strategy may have high background noise that would affect the sensitivity; this hampers the wide applications of this strategy.

In this study, we developed a "turn-on" fluorescence assay for monitoring the 3′–5′ exonuclease enzymatic activity based on the interaction between GO and a DNA hairpin probe (HP). The developed assay showed an ultra-low limit of detection of 0.001 U mL^{-1} in buffer and 0.004 U mL^{-1} in a 25-times diluted serum sample. This highly sensitive and selective assay provides a promising new technology for the monitoring of 3′–5′ exonuclease enzymatic activity in clinical diagnosis.

Experimental

Chemicals and materials

Graphene oxide aqueous solution (5 mg mL^{-1}) was purchased from ACS Material (Pasadena, CA). The sequence of hairpin probe (HP) was 5′-TTTTTTTTTTGGATCCCGCTTCTTTTTTTTT-TGAAGCGGGATCC-FAM-3′, which was synthesized by the Integrated DNA Technologies (IDT). Exonuclease III (Exo III), T4 polynucleotide kinase (T4 PNK), alkaline phosphatase, calf intestinal phosphatase (CIP), uracil-DNA glycosylase (UDG), exonuclease I (Exo I), RecJf, lambda exonuclease (Lambda Exo) and 10× NEBuffer 2 were obtained from the New England Biolabs (NEB). PBS tablets and ethylenediaminetetraacetic acid were purchased from Sigma Aldrich, Inc. The biological sample (fetal bovine serum) obtained from the School of Medicine & Health Science, University of North Dakota, was also purchased from Sigma Aldrich, Inc. Deionized (DI) water (18.2 MΩ cm) was produced using a Millipore water purification system.

Apparatus

Fluorescence measurements were performed using the RF-6000 fluorophotometer (SHIMADZU, Kyoto, Japan). The excitation wavelength was set to be 480 nm, and the emission was recorded from 500 nm to 650 nm. The fluorescence intensity at 517 nm was selected to evaluate the performance of Exo III detection. The width of both the excitation and the emission slits was 10 nm. All the experiments were carried out at 37 °C. The morphology and the element analysis of GO were carried out using the Hitachi SU8010 field-emission scanning electron microscope (SEM) equipped with an energy-dispersive X-ray spectrometer.

Feasibility of the sensor for Exo III detection

A 100 μL aliquot of 1× NEBuffer 2 containing 100 nM hairpin probe (HP) was mixed with 1 μL of 50 U mL^{-1} Exo III and then incubated at 37 °C for 10 min. Then, 1 μL of 2 mg mL^{-1} GO solution was added and incubated at 37 °C for another 10 min. The fluorescence spectra of the solution were recorded at an excitation wavelength of 480 nm.

Detection of Exo III activity

Briefly, a 100 μL aliquot of 1× NEBuffer 2 containing 100 nM hairpin probe (HP) was mixed with 1 μL of various concentrations of Exo III and then incubated at 37 °C for 10 min. Then, 1 μL of 2 mg mL^{-1} GO was added to the above solution and incubated at 37 °C for another 10 min. The fluorescence intensity of the final solution was detected at an excitation wavelength of 480 nm.

Evaluation of the selectivity

The selectivity of the assays was evaluated by testing the fluorescence signal of the sensing system to other DNA digesting enzymes. Typically, a whole volume of 100 μL solution containing HP (100 nM) and 10 U mL^{-1} of one of the following enzymes, including Exo III, Exo I, Lambda Exo, RecJf, T4 PNK, CIP and UDG, was incubated in a 37 °C water bath for 10 min. Then, 1 μL of 2 mg mL^{-1} GO was mixed with the above solution and incubated at 37 °C for an additional 10 min. The fluorescence intensity was measured at an excitation wavelength of 480 nm.

Exonuclease inhibition assay

To perform the inhibition assay on the activity of Exo III, a 100 μL aliquot of solution containing 10 U mL^{-1} Exo III, 100 nM HP and various concentrations of EDTA was incubated at 37 °C for 10 min, followed by the addition of 1 μL of 2 mg mL^{-1} GO and incubated for another 10 min in a 37 °C water bath. The fluorescence intensity of the final solution was determined at an excitation wavelength of 480 nm.

Performance in 25-times diluted serum

A 0.4 mL volume of fetal bovine serum sample was added to 0.6 mL of acetonitrile. The mixture was stirred through a vigorous vortex for 5 and then centrifuged at 10 000 rpm for 10 min. The collected supernatant was diluted by 5 times with 1× NEBuffer 2. To test the Exo III activity, a 100 μL aliquot of the above 5-times diluted FBS sample was first mixed with 100 μL of 200 nM HP, followed by the addition of different concentrations of Exo III (0, 0.01, 0.05, 0.10, 0.15, 0.5, 1.0, and 5.0 U mL^{-1}). The abovementioned solution was then incubated in a 37 °C water bath for 10 min. Finally, a 2 μL of 2 mg mL^{-1} GO was added into the previous solution and incubated for another 10 min in a 37 °C water bath. The fluorescence spectra were obtained at an excitation wavelength of 480 nm.

Kinetic analysis

In general, a 100 μL aliquot of 1× NEBuffer 2 containing 100 nM hairpin probe (HP) was mixed with 1 μL of 2 mg mL^{-1} GO. The fluorescence at 517 nm with excitation at 480 nm was recorded with time. After the fluorescence was stabilized, 1 μL of various concentrations of Exo III was added and incubated at 37 °C. The fluorescence intensity was monitored *vs.* time for another 5 min.

Results and discussion

Design of the Exo III assay

As shown in Scheme 1, a hairpin probe (HP) modified with a fluorophore (FAM) at the blunt 3′-termini was used for this sensor. The intact FAM tapped HP without the treatment of Exo III would be strongly absorbed onto GO due to the strong π–π stacking interaction between them, leading to absolute fluorescence quenching through the efficient FRET (Pathway a). However, when Exo III was present, it digested the phosphoric-ester bonds and removed the mononucleotides starting from the blunt 3′-termini of HP to the whole double strand domain, generating a long unlabeled ssDNA and an FAM-labeled mononucleotide. With the addition of GO, the ssDNA absorbed onto GO spontaneously but the affinity between the FAM-labeled mononucleotide and GO was much weaker than that observed with ssDNA.[31] Because of the dissociation between the GO and FAM-labeled mononucleotides (Pathway b), fluorescence was significantly restored when compared with the case of the sample without the Exo III treatment.

Characterization of GO

In this sensor, we utilized GO as a quencher due to its excellent quenching efficiency to various fluorophores and its different affinities to ssDNA and mononucleotides.[32] To characterize the morphology of GO and elemental analysis, an SEM image of GO and the corresponding energy-dispersive X-ray spectroscopy mapping were obtained (Fig. 1). The average size of the GO sheets was around 800 nm, which provided larger surface area for ssDNA (loop domain) attachment (Fig. 1A). The EDS analysis showed that GO mostly contained the elements carbon and oxygen (Fig. 1B and C). Moreover, the absorption spectrum of GO showed a typical peak at 230 nm of GO and broad absorption from UV to visible range (Fig. 1E), making GO an ideal fluorescence quencher for a variety of fluorophores.

Feasibility investigation

To demonstrate the feasibility of the developed sensor, the fluorescence emission spectra of the HP under different conditions were obtained. As shown in Fig. 2, pure HP (100 nM) emitted fluorescence at 517 nm with the excitation wavelength of 480 nm (curve a). When GO was added to the HP, the fluorescence intensity rapidly decreased by over 95% (curve b), indicating the super fluorescence quenching ability of GO. In contrast, when HP was treated with Exo III before the addition of GO, a relatively high fluorescence intensity was obtained (curve c), which was attributed to the removal of the FAM-labelled blunt 3′-termini part out of HP by Exo III, enhancing the distance and weakening the FRET between GO and FAM. The variation of the three spectra confirmed that this sensing system could be applied for the detection of Exo III activity.

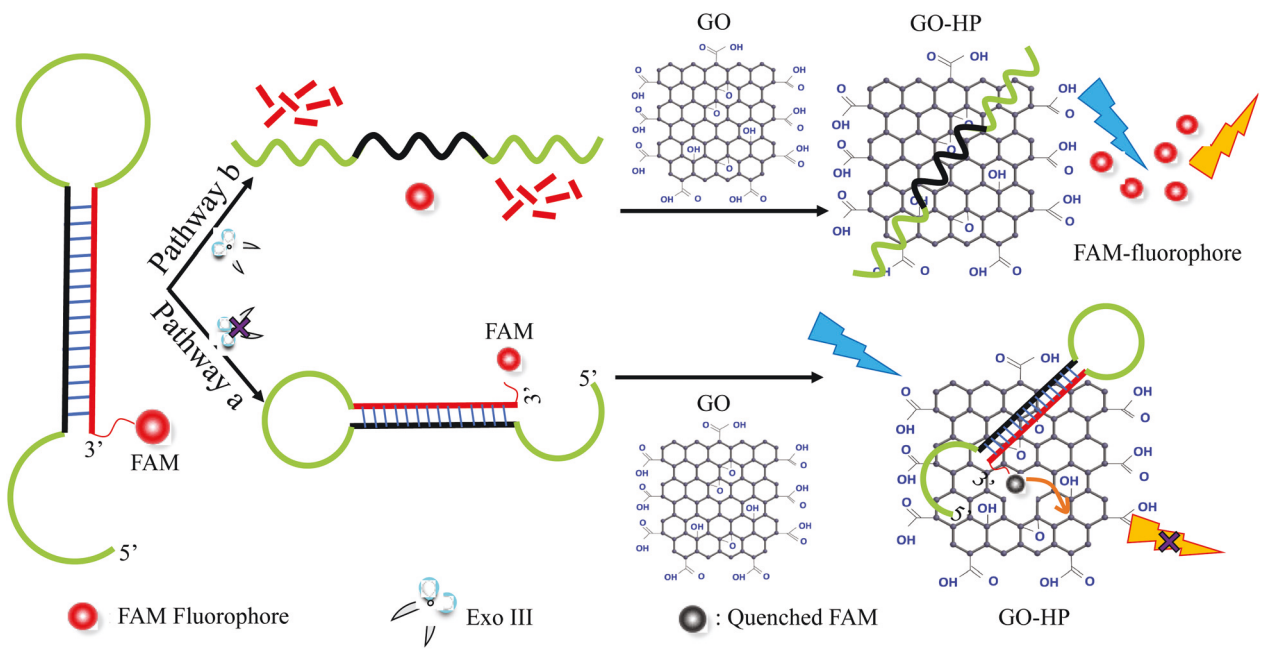

Scheme 1 Schematic of the Exo III detection based on the GO and FAM-labelled HP.

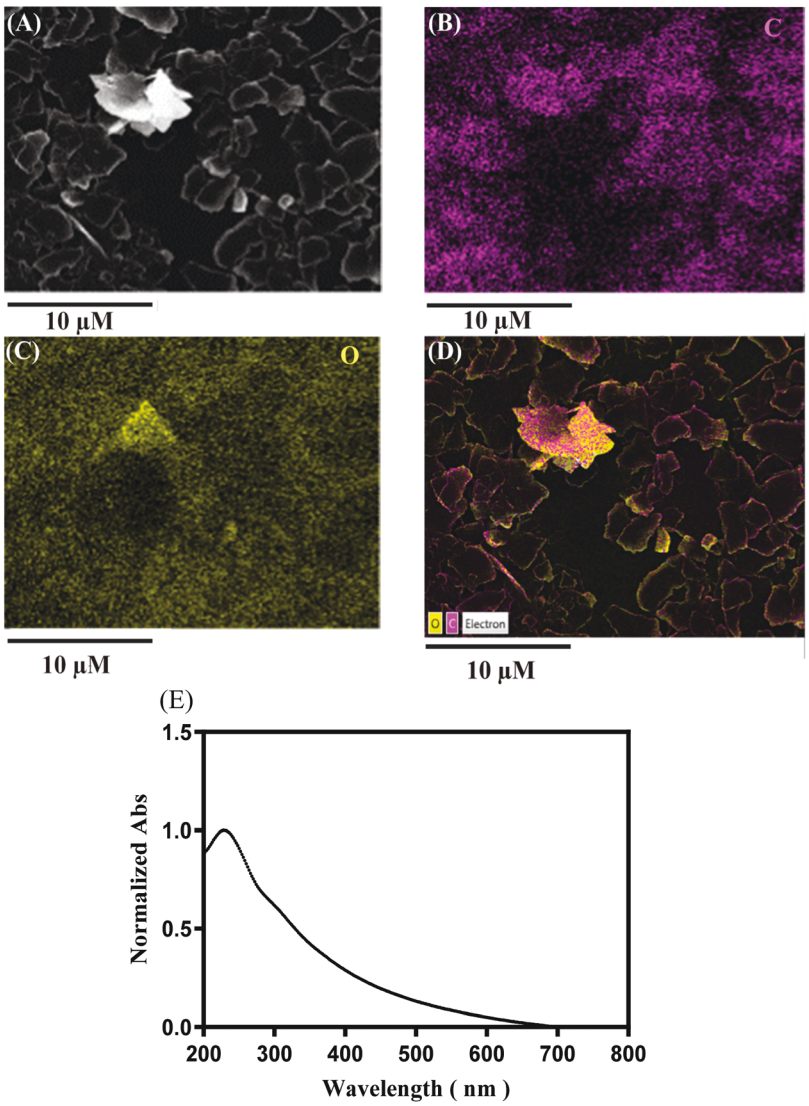

Fig. 1 (A) The SEM image and the corresponding elemental maps of GO: (B) carbon (pink) and (C) oxygen (yellow); (D) overlayered mapping of GO (scale bar = 10 μm); (E) UV–vis absorption spectrum of GO with a typical absorption maximum at 230 nm.

Optimization of experimental conditions

To determine the optimal conditions for Exo III activity analysis, the impacts of the concentration of GO, the concentration of HP, and the reaction time on the sensing performance were investigated. As shown in Fig. 3A, a time-based fluorescence collection was performed with a whole volume of 100 μL solution (containing 20 μg mL^{-1} GO and 50 nM HP in 1× NEBuffer2) at 37 °C for 1200 s. After the addition of GO, the fluorescence intensity decreased substantially in the first 100 s and then reached a plateau after about 200 s. Therefore, the reaction time in the quenching process was set to 10 min.

Moreover, the concentration of GO needed to be considered to reach a low background. The fluorescence intensity of HP with and without different concentrations of GO was measured to assess the optimal concentration of GO. As shown in Fig. 3B, F_0 refers to the fluorescence intensity of 100 nM HP without GO, and F refers to the fluorescence intensity of 100 nM HP after the addition of various concentrations of GO. The ratio of F/F_0 decreased as the concentration of GO increased, indicating the concentration-dependent quenching ability of GO. The ratio reached a plateau after the concentration was enhanced to 20 μg mL^{-1}. Therefore, in the following experiments, we used 20 μg mL^{-1} as the optimal concentration of GO to perform the subsequent detection.

The concentration of HP was the third impact that needed to be optimized. A series of concentrations of HP were incubated with 50.0 U mL^{-1} Exo III, followed by mixing with 20 μg mL^{-1} GO (Fig. 4). Fluorescence intensity of the abovementioned solution was obtained and designated as F. In contrast, another series of the same concentrations of HP was directly mixed with 20 μg mL^{-1} GO only, whose fluorescence intensity was defined as F_0. The corresponding ratios of F to F_0 reached a maximum value at the concentration of 100 nM of HP,

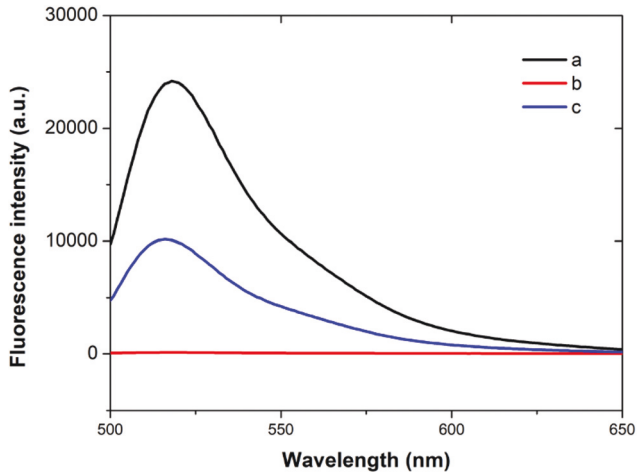

Fig. 2 Fluorescence spectra of HP (100 nM) under different conditions. (a) 100 nM HP; (b) 100 nM HP + 20 μg mL^{-1} GO; and (c) 100 nM HP + 0.5 U mL^{-1} Exo III + 20 μg mL^{-1} GO; λ_{ex} = 480 nm, all of the reagents were incubated in 1× NEBuffer 2; and λ_{em} = 500–650 nm.

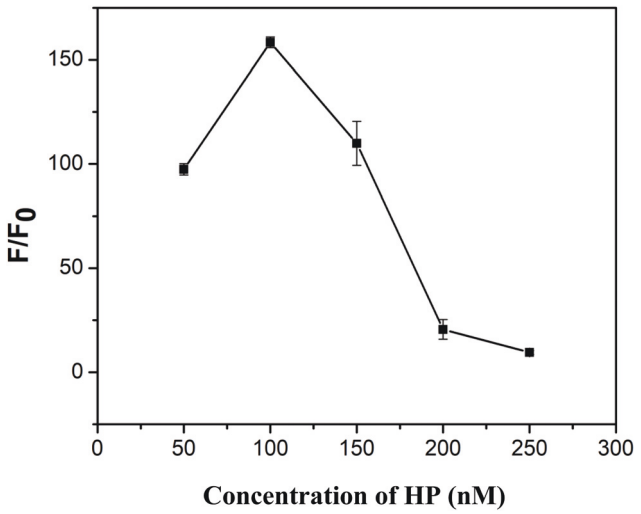

Fig. 4 The effect of the concentration of HP on the performance of the sensor. F refers to the fluorescence intensity of the different concentrations of HP treated with 50 U mL^{-1} of Exo III followed by the addition of 20 μg mL^{-1} GO. F_0 represents the fluorescence intensity of the same series of HP without the treatment of Exo III but in the presence of 20 μg mL^{-1} GO. λ_{ex} = 480 nm and λ_{em} = 517 nm.

suggesting highest sensitivity at this concentration. Consequently, we set the concentration of HP to 100 nM for the following experiments.

Exo III detection

To investigate the sensitivity of the sensor towards Exo III, a 100 nM HP solution was treated with different concentrations of Exo III for 10 min at 37 °C, followed by the addition of 20 μg mL^{-1} GO. As shown in Fig. 5A, the fluorescence intensity of FAM increased when the concentration of Exo III was increased from 0 U mL^{-1} to 20.0 U mL^{-1}. The results showed that the dynamic range was from 0 U mL^{-1} to 20.0 U mL^{-1} (Fig. 5B), with a linear range between 0.01 U mL^{-1} and 0.5 U mL^{-1} (the inset of Fig. 5B). The calibration curve showed a regression equation of $Y = 19380.6X + 71.6$, with a correlation coefficient of 0.9855. Y and X represented the fluorescence intensity and the concentration of Exo III in unit of U mL^{-1}, respectively. The limit of detection (LOD) for the detection of Exo III was calculated to be 0.001 U mL^{-1} based on the slope of the equation ($3\sigma/s$), where σ was the standard deviation of the four blank fluorescence intensities and s was the slope of the calibration curve. This ultra-low LOD demonstrates that the GO-based sensor is an ultra-sensitive platform for the detection of Exo III activity when compared with the other

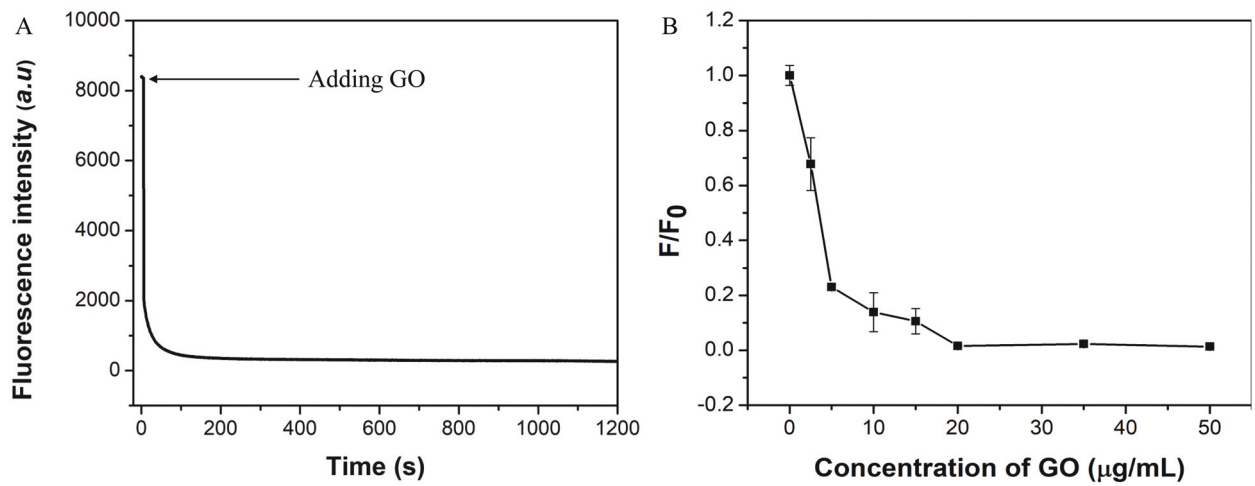

Fig. 3 (A) A time-based fluorescence intensity curve was collected in a 100 μL 1× NEBuffer2 solution containing 50 nM HP solution with the addition of 20 μg mL^{-1} GO at 37 °C for 1200 s. (B) Fluorescence intensity ratios of F/F_0 at different concentrations of GO. F_0 refers to the fluorescence intensity of 100 nM HP without GO, and F refers to the fluorescence intensity of 100 nM HP after the addition of various concentrations of GO. λ_{ex} = 480 nm and λ_{em} = 517 nm.

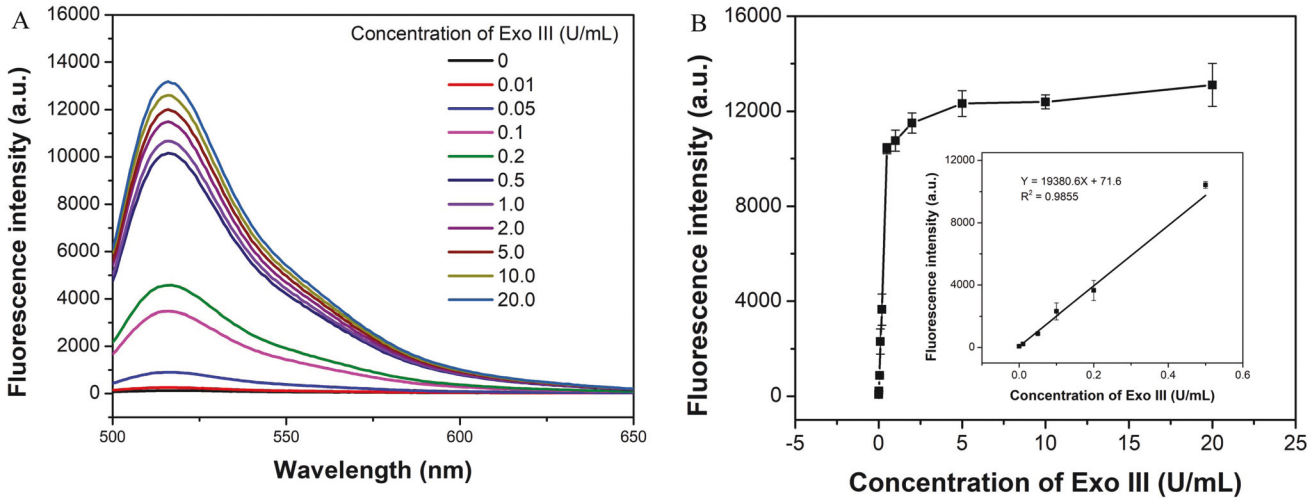

Fig. 5 (A) Fluorescence spectra of the sensor incubated with different concentrations of Exo III (from 0 U mL^{-1} to 20.0 U mL^{-1}). (B) The plot of the fluorescence intensity with different concentrations of Exo III. The inset graph shows the calibration curve of the sensor. Reaction conditions: 100 nM HP and 20 μg mL^{-1} GO in 100 μL 1× NEBuffer 2. λ_{ex} = 480 nm and λ_{em} = 517 nm.

Table 1 Comparison of the proposed sensor with other fluorescent methods

Probes	LOD (U mL^{-1})	Linear range	Response time	Ref.
Molecular beacons	0.01	0.04–8 U mL^{-1}	200 s	19
Copper nanoparticles	0.02	0.05–2 U mL^{-1}	91 min	33
SYBI green I	0.7	1–200 U mL^{-1}	110 min	34
G-Quadruplex	0.8	5–100 U mL^{-1}	70 min	17
GO/HP	0.001	0.01–0.5 U mL^{-1}	20 min	This work

fluorescence methods (Table 1). Moreover, the present study only needed one-termini modification of the DNA probe when compared with our previous studies with molecular beacon, and the superior quenching ability of GO significantly decreased the background, thus enhancing the sensitivity of the sensor.

Selectivity investigation

To validate the selectivity of this sensor, we studied the response of the sensor towards a series of DNA enzymes, including Exo I, T4 PNK, Lambda Exo, RecJf, CIP, UDG and Exo III, with a concentration of 10 U mL^{-1}. Exo I enzyme cuts down the single-stranded DNA from the 3′ termini to 5′ termini.[35] Lambda Exo removes the 5′ mononucleotides from duplex DNA.[36] RecJf digests single-stranded DNA specifically from 5′ termini to 3′ termini.[37] T4 PNK hunts for the 5′ phosphorylation of DNA/RNA for subsequent ligation.[38] CIP catalyses the dephosphorylation of 5′ and 3′ ends of DNA and RNA.[39] UDG is a recombinant enzyme that releases uracil from single-stranded or double-stranded DNA.[40] These DNA enzymes are very common and play essential roles in multiple biological processes. Therefore, it was important to determine the selectivity of the senor for Exo III enzymatic activity. As shown in Fig. 6, with the same concentration treatment of

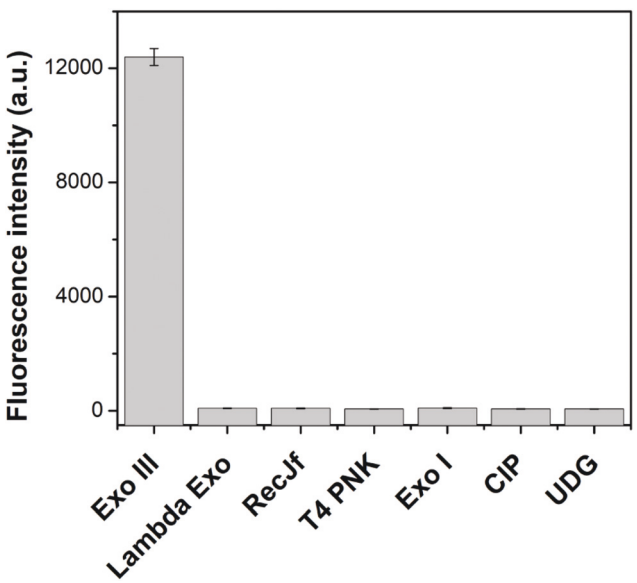

Fig. 6 Selectivity of the sensor for Exo III over other enzymes. Reaction conditions: 100 nM HP and 20 μg mL^{-1} GO in 100 μL 1× NEBuffer 2. The concentration of the enzyme was 10 U mL^{-1}. λ_{ex} = 480 nm and λ_{em} = 517 nm.

these enzymes, only Exo III caused a significant fluorescence enhancement when compared with the other enzymes. These results demonstrate that this sensor has excellent selectivity for Exo III detection.

Inhibition test

We further evaluated the inhibition assay of Exo III as it was important for drug screening. EDTA, as a chelating agent, could effectively inhibit the activity of Exo III.[41] As shown in Fig. 7, the fluorescence intensity of the sensor decreased with

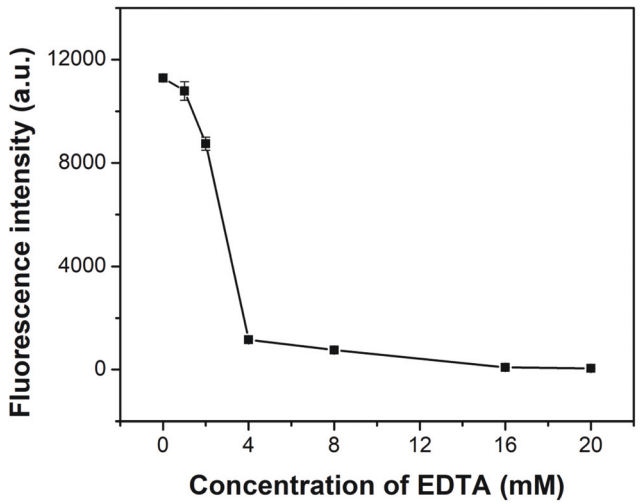

Fig. 7 Effect of EDTA concentration on the Exo III activity. Reaction conditions: 100 nM HP and 20 μg mL^{-1} GO in 100 μL 1× NEBuffer 2. The concentration of Exo III was 10 U mL^{-1}. λ_{ex} = 480 nm and λ_{em} = 517 nm.

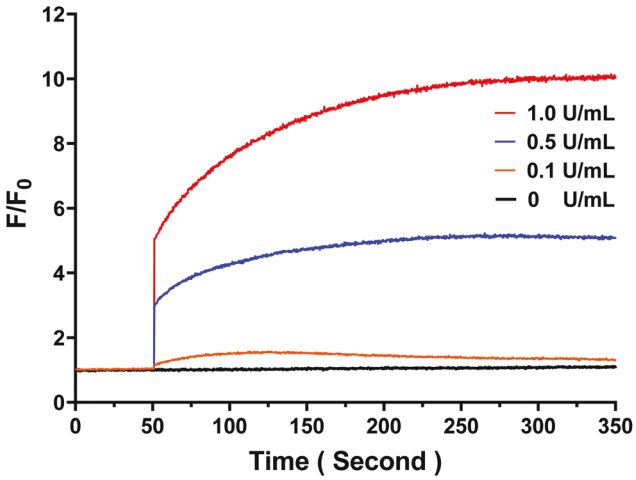

Fig. 9 Real-time kinetic analysis of Exo III with different concentrations. From bottom to top: 0, 0.1, 0.5, 1 U mL^{-1}.

an increase in the concentration of EDTA, indicating the inhibition effect of EDTA for Exo III activity. Half-maximal inhibitory concentration (IC_{50}) of EDTA was estimated to be 3.0 mM. The results demonstrated that this designed sensor could be utilized for drug screening specifically for selecting the potential inhibitors of Exo III activity.

Application in diluted serum samples

To test the applicability of the sensor, we investigated the performance of the sensor in fetal bovine serum (FBS). The experiments were conducted under the same optimized conditions, except that the 1× NEBuffer 2 was replaced with 10-times diluted FBS with buffer. Similarly, the fluorescence intensity of FAM increased as the concentration of Exo III was increased from 0 U mL^{-1} to 5.0 U mL^{-1} (Fig. 8), with a linear range between 0.01 U mL^{-1} and 0.15 U mL^{-1} (the inset of Fig. 8B). The calibration curve showed a regression equation of Y = 14.388X + 1.157 with a correlation coefficient of 0.9741. Y and X represented the fluorescence intensity and the concentration of Exo III in the unit of U mL^{-1}, respectively. The limit of detection (LOD) for Exo III was calculated to be 0.004 U mL^{-1} in 25-times diluted FBS based on the slope of the equation ($3\sigma/s$). The results suggested that the sensor could be used in complicated samples for the detection of the enzymatic activity of Exo III.

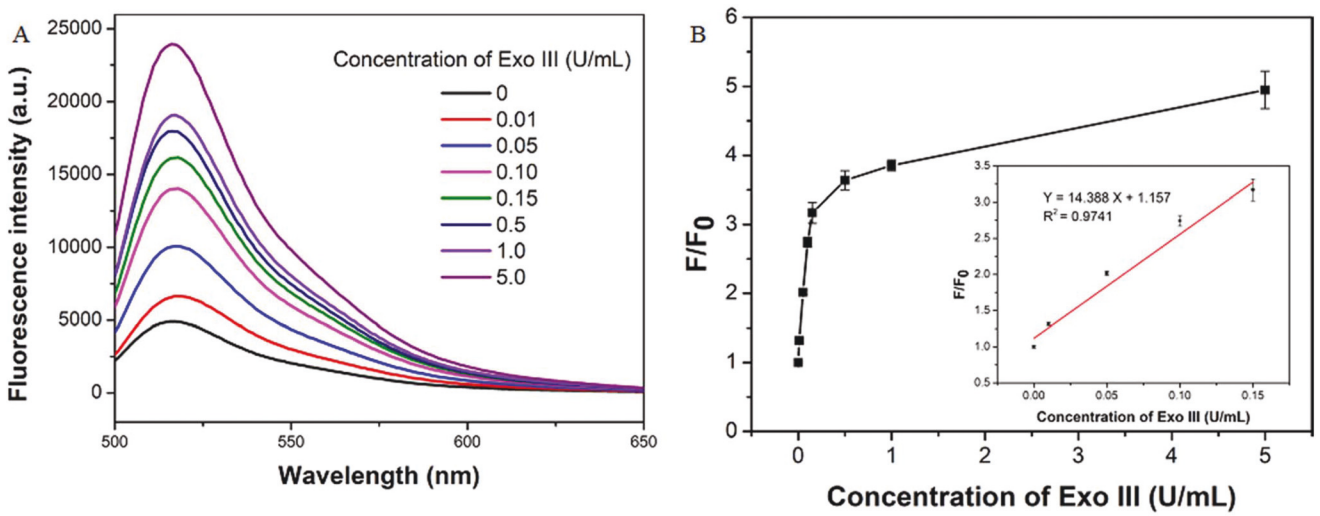

Fig. 8 (A) Fluorescence spectra of the sensor upon incubation with different concentrations of Exo III in 25-times diluted FBS from 0 to 5 U mL^{-1}. (B) The plot of the fluorescence intensity with different concentrations of Exo III. The inset graph shows the calibration curve of the sensor. Reaction conditions: 100 nM HP and 20 μg mL^{-1} GO in 200 μL 25-times diluted FBS. λ_{ex} = 480 nm and λ_{em} = 517 nm.

Kinetic analysis

To conduct the kinetic analysis of the enzymatic activity, we performed the real-time fluorescence measurements using the sensor for different concentrations of Exo III. As shown in Fig. 9, the fluorescence of HP was first totally quenched by the addition of GO, indicating a strong interaction between GO and HP, as well as the excellent quenching ability of GO towards the fluorophore. When the fluorescence intensity was stabilized, an aliquot of Exo III with different concentrations was introduced into the cuvette. The immediate fluorescence obtained showed a dramatic fluorescence enhancement after the addition of Exo III, indicating a rapid enzymatic reaction in the sensor. The signal-to-background ratio reached about 10.0 when the concentration of Exo III was 1.0 U mL^{-1}. The fluorescence intensity reached a plateau after about 300 s.

Conclusion

In conclusion, we developed a simple and ultra-sensitive fluorescent sensor to detect the enzymatic activity of Exo III. The design was based on the different affinities of ssDNA and mononucleotide with GO and the superior quenching ability of GO to fluorophores. The sensor presented excellent selectivity to Exo III with the LOD of 0.001 U mL^{-1} in buffer and 0.004 U mL^{-1} in 25-times diluted FBS. To the best of our knowledge, the LOD obtained in this assay is superior to that obtained in the fluorescent methods for Exo III detection; the successful application of the sensor in a complex sample (diluted serum) suggests that this method has the potential to be used for disease diagnosis and drug screening based on enzymatic activity.

Conflicts of interest

There are no conflicts to declare.

Acknowledgements

This work was supported by the NSF CHE 1709160, University of North Dakota Postdoctoral Pilot Program supported by the UND VPR and Art and Science College, the North Dakota Industrial Commission Grant G-041-081, and the Applied Research to Address the State's Critical Needs Initiative program.

References

1 P. A. Mason and L. S. Cox, *Age*, 2012, **34**, 1317–1340.
2 S. G. Rogers and B. Weiss, [26] Exonuclease III of Escherichia coli K-12, an AP endonuclease, in *Methods in Enzymology*, Academic Press, 1980, vol. 65, pp. 201–211.
3 L. L. Souza, I. R. Eduardo, M. Pádula and A. C. Leitão, *Mutagenesis*, 2006, **21**, 125–130.
4 I. J. Fijalkowska and R. M. Schaaper, *Proc. Natl. Acad. Sci. U. S. A.*, 1996, **93**, 2856–2861.
5 T. T. Paull and M. Gellert, *Mol. Cell*, 1998, **1**, 969–979.
6 A. M. Whitaker, T. S. Flynn and B. D. Freudenthal, *Nat. Commun.*, 2018, **9**, 399.
7 Y.-C. Chen, C.-L. Li, Y.-Y. Hsiao, Y. Duh and H. S. Yuan, *Nucleic Acids Res.*, 2014, **42**, 10776–10785.
8 I. V. Shevelev and U. Hübscher, *Nat. Rev. Mol. Cell Biol.*, 2002, **3**, 364–376.
9 D. Kavanagh, D. Spitzer, P. Kothari, A. Shaikh, M. K. Liszewski, A. Richards and J. P. Atkinson, *Cell Cycle*, 2008, **7**, 1718–1725.
10 C.-J. Wang, W. Lam, S. Bussom, H.-M. Chang and Y.-C. Cheng, *DNA Repair*, 2009, **8**, 1179–1189.
11 M. Brucet, J. Querol-Audí, K. Bertlik, J. Lloberas, I. Fita and A. Celada, *Protein Sci.*, 2009, **17**, 2059–2069.
12 A. V. Nimonkar, A. Z. Ozsoy, J. Genschel, P. Modrich and S. C. Kowalczykowski, *Proc. Natl. Acad. Sci. U. S. A.*, 2008, **105**, 16906–16911.
13 D. A. Lehtinen, S. Harvey, M. J. Mulcahy, T. Hollis and F. W. Perrino, *J. Biol. Chem.*, 2008, **283**, 31649–31656.
14 J. Lee and D.-H. Min, *Analyst*, 2012, **137**, 2024–2026.
15 P. Zou, Y. Liu, H. Wang, J. Wu, F. Zhu and H. Wu, *Biosens. Bioelectron.*, 2016, **79**, 29–33.
16 N. Dai and E. T. Kool, *Chem. Soc. Rev.*, 2011, **40**, 5756–5770.
17 W. Yang, Y. Ruan, W. Wu, P. Chen, L. Xu and F. Fu, *Anal. Bioanal. Chem.*, 2014, **406**, 4535–4540.
18 Q. Xu, Y. Zhang and C.-y. Zhang, *Chem. Commun.*, 2015, **51**, 9121–9124.
19 X. Wu, J. Chen and J. X. Zhao, *Analyst*, 2014, **139**, 1081–1087.
20 Y. Wang, Z. Li, J. Wang, J. Li and Y. Lin, *Trends Biotechnol.*, 2011, **29**, 205–212.
21 Y. Zhu, S. Murali, W. Cai, X. Li, J. W. Suk, J. R. Potts and R. S. Ruoff, *Adv. Mater.*, 2010, **22**, 3906–3924.
22 R. K. Singh, R. Kumar and D. P. Singh, *RSC Adv.*, 2016, **6**, 64993–65011.
23 F. Liu, J. Y. Choi and T. S. Seo, *Biosens. Bioelectron.*, 2010, **25**, 2361–2365.
24 E. Morales-Narváez and A. Merkoçi, *Adv. Mater.*, 2012, **24**, 3298–3308.
25 Y. Liu, C.-y. Liu and Y. Liu, *Appl. Surf. Sci.*, 2011, **257**, 5513–5518.
26 A. Kasry, A. A. Ardakani, G. S. Tulevski, B. Menges, M. Copel and L. Vyklicky, *J. Phys. Chem. C*, 2012, **116**, 2858–2862.
27 H. Dong, W. Gao, F. Yan, H. Ji and H. Ju, *Anal. Chem.*, 2010, **82**, 5511–5517.
28 C. Liu, Z. Wang, H. Jia and Z. Li, *Chem. Commun.*, 2011, **47**, 4661–4663.
29 J. Shi, J. Guo, G. Bai, C. Chan, X. Liu, W. Ye, J. Hao, S. Chen and M. Yang, *Biosens. Bioelectron.*, 2015, **65**, 238–244.
30 S. Li, A. N. Aphale, I. G. Macwan, P. K. Patra, W. G. Gonzalez, J. Miksovska and R. M. Leblanc, *ACS Appl. Mater. Interfaces*, 2012, **4**, 7069–7075.
31 F. Li, Y. Feng, C. Zhao, P. Li and B. Tang, *Chem. Commun.*, 2012, **48**, 127–129.

32 X. Wu, Y. Xing, K. Zeng, K. Huber and J. X. Zhao, *Langmuir*, 2018, **34**, 603–611.
33 H. Zhang, Z. Lin and X. Su, *Talanta*, 2015, **131**, 59–63.
34 M. Xu and B. Li, *Spectrochim. Acta, Part A*, 2015, **151**, 22–26.
35 I. R. Lehman and A. L. Nussbaum, *J. Biol. Chem.*, 1964, **239**, 2628–2636.
36 P. G. Mitsis and J. G. Kwagh, *Nucleic Acids Res.*, 1999, **27**, 3057–3063.
37 S. T. Lovett and R. D. Kolodner, *Proc. Natl. Acad. Sci. U. S. A.*, 1989, **86**, 2627–2631.
38 C. C. Richardson, 16 Bacteriophage T4 Polynucleotide Kinase, in *The Enzymes*, ed. P. D. Boyer, Academic Press, 1981, vol. 14, pp. 299–314.
39 M. R. Green and J. Sambrook, in *Molecular Cloning: A Laboratory Manual*, Cold Spring Harbor Laboratory Press, 4th edn, 1980, vol. 2, p. 1009.
40 T. Lindahl, S. Ljungquist, W. Siegert, B. Nyberg and B. Sperens, *J. Biol. Chem.*, 1977, **252**, 3286–3294.
41 R. C. B. Silva-Portela, F. M. Carvalho, C. P. M. Pereira, N. C. de Souza-Pinto, M. Modesti, R. P. Fuchs and L. F. Agnez-Lima, *Sci. Rep.*, 2016, **6**, 19712–19712.